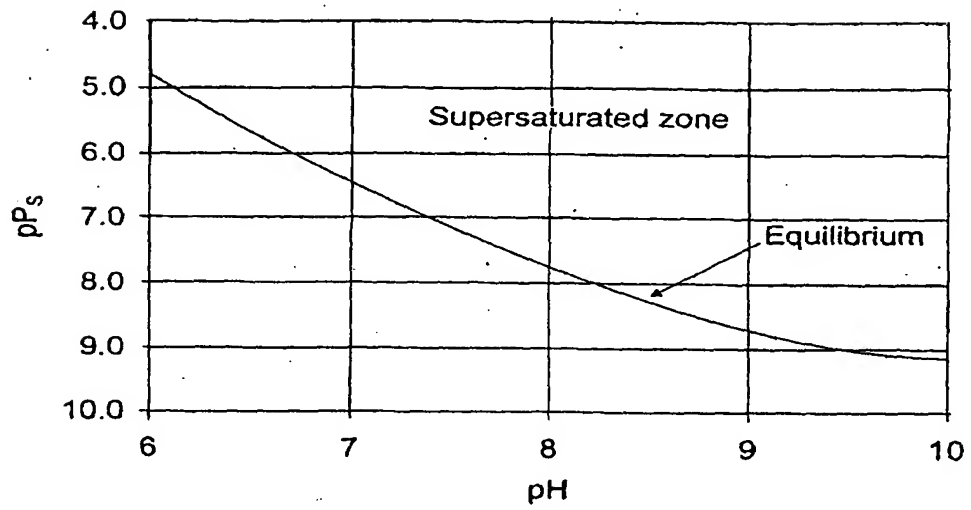

Figure 1: Variation of Equilibrium Conditional Solubility versus pH for Struvite (from Ohlinger et al., 1998)

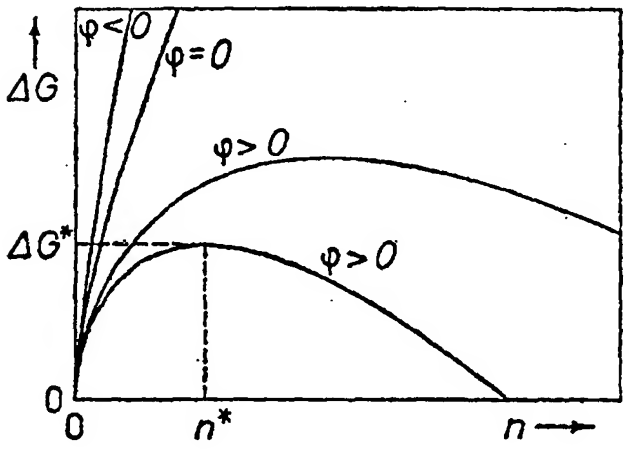

Figure 2: Free Energy versus Number of Particles in a Precipitating Crystal

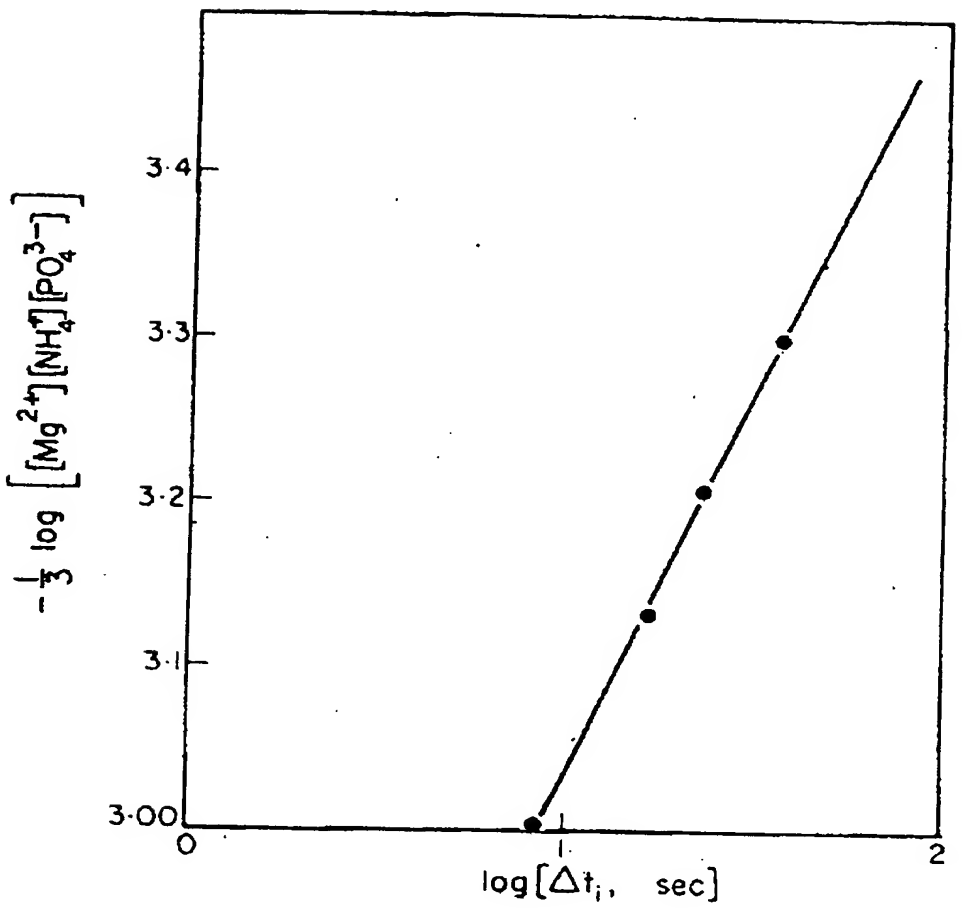

Figure 3: Concentration (-1/3 log of Ionic Product, Mol/L) versus Induction Time (Sec) for Struvite Precipitation

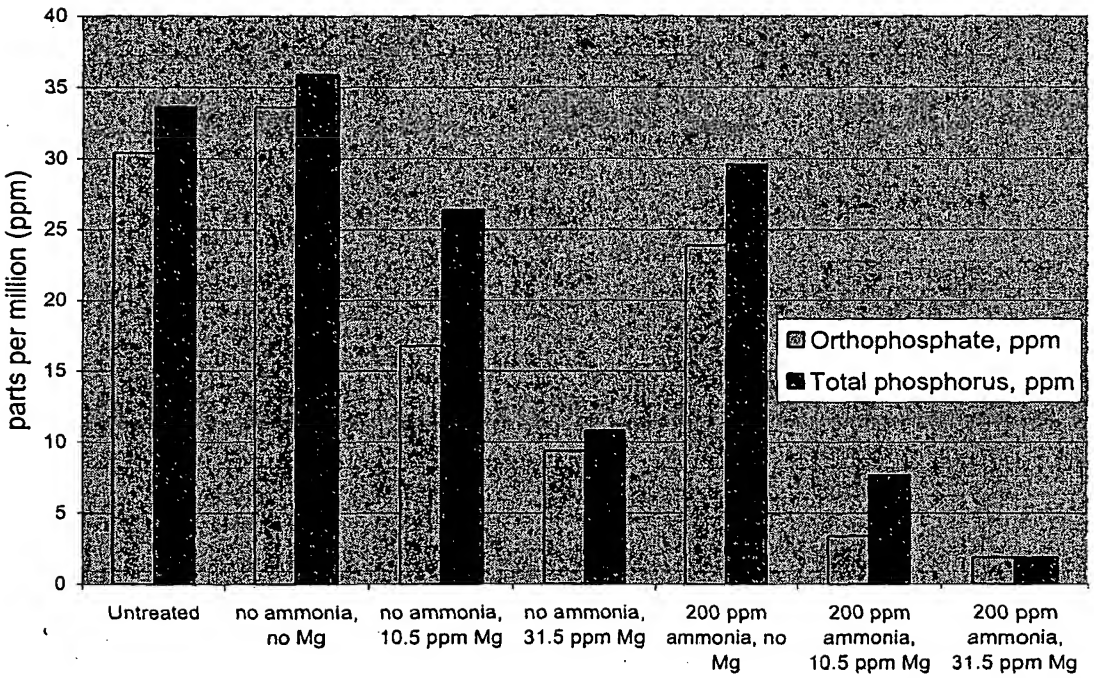

Figure 4: Dissolved OP and TP (ppm) in Untreated and Treated Effluent from Rocky Mount Lagoon

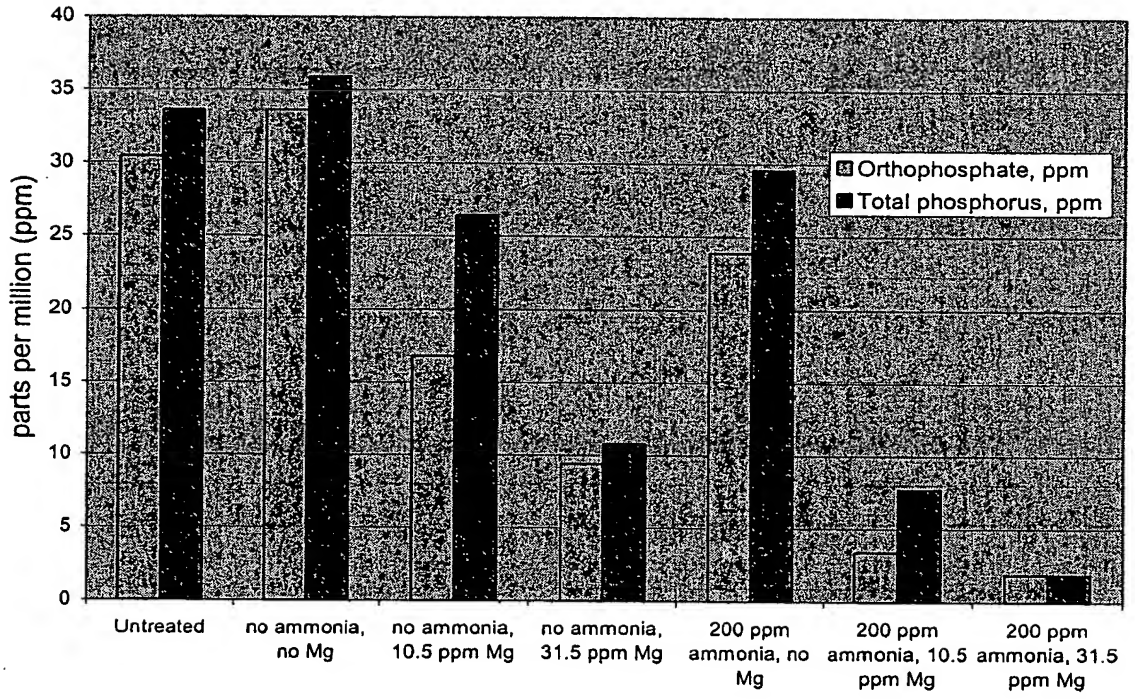

Figure 5: Dissolved OP and TP (ppm) in Untreated and Treated Effluent from Clayton Digester

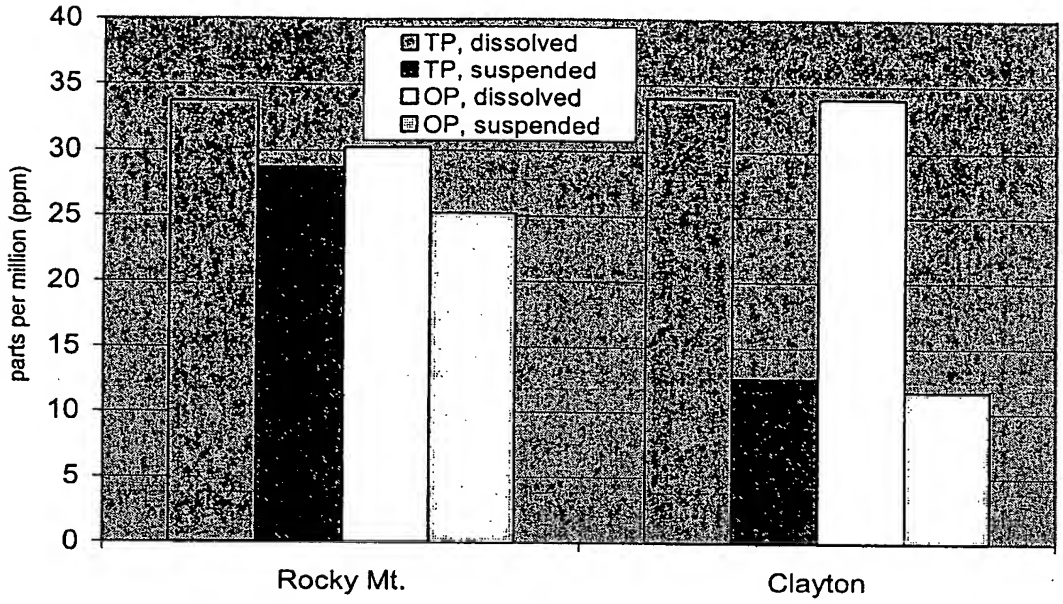

Figure 6: Breakdown of Phosphorus Content (ppm) by Form in Rocky Mount and Clayton Effluent

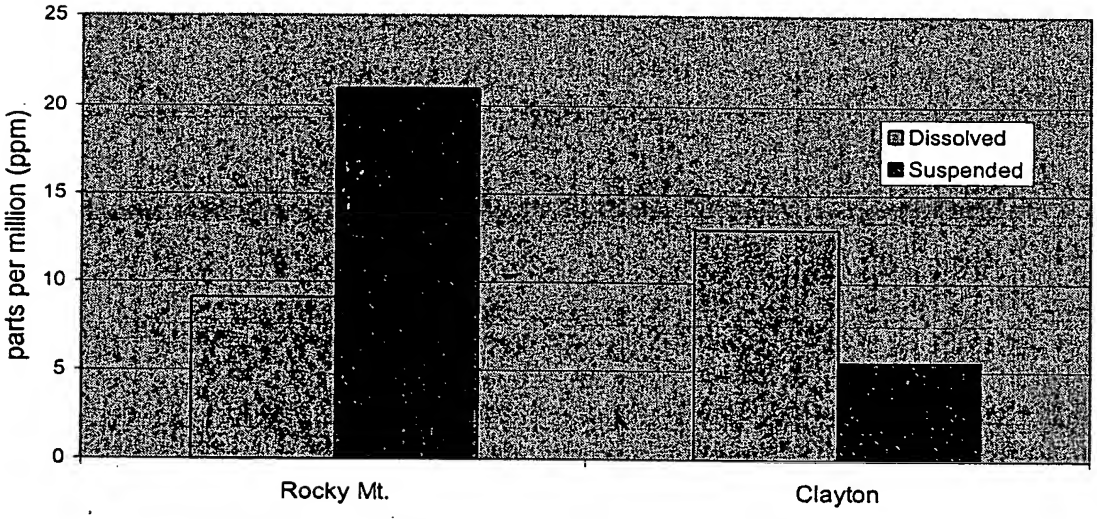

Figure 7: Breakdown of Mg Content (ppm) by Form in Rocky Mount and Clayton Effluents

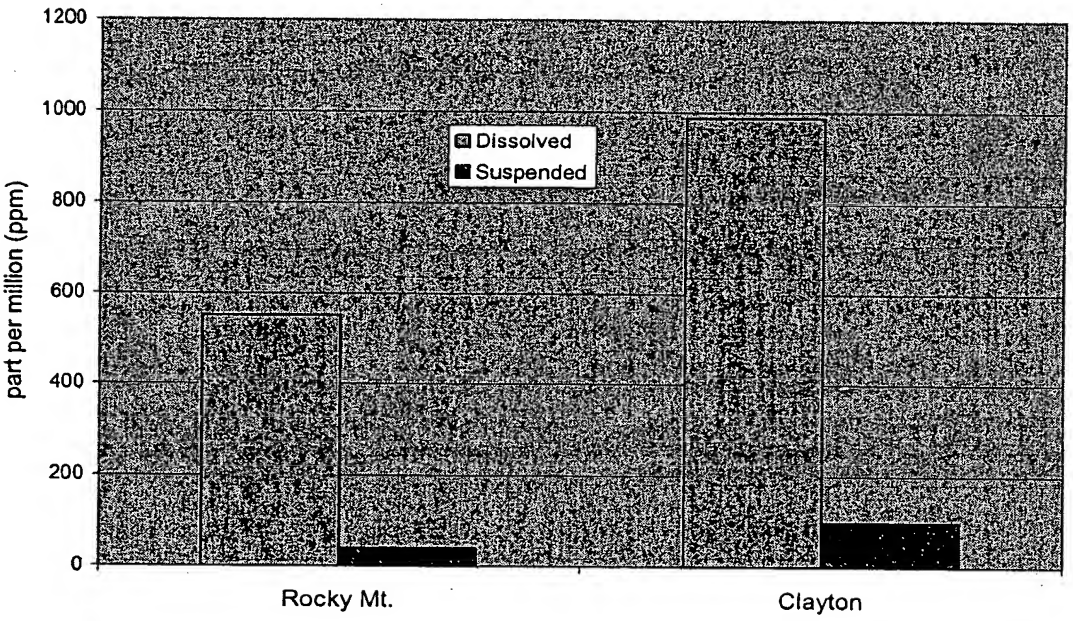

Figure 8: Breakdown of TAN (ppm) by Form in Rocky Mount and Clayton Effluent

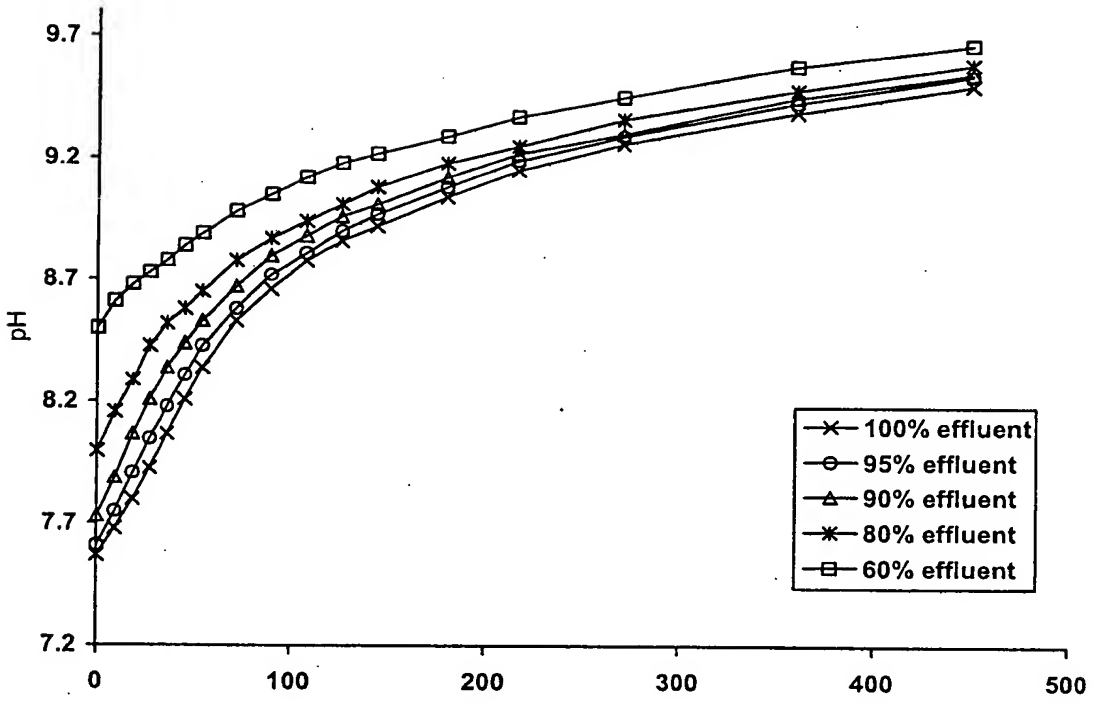

Figure 9: pH versus Amount of Ammonia Added (ppm) for Five Ratios of Effluent to Mg-Supplementing Solution

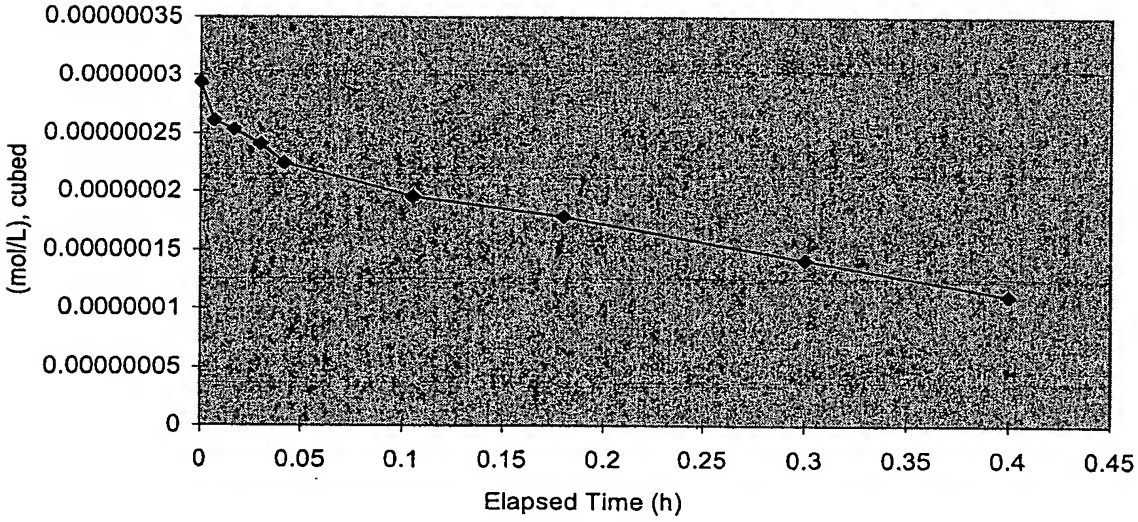

Figure 10: Excess Molar Product $(mol/L)^3$ versus Time (h) Elapsed from pH, OP, and Mg Augmentation

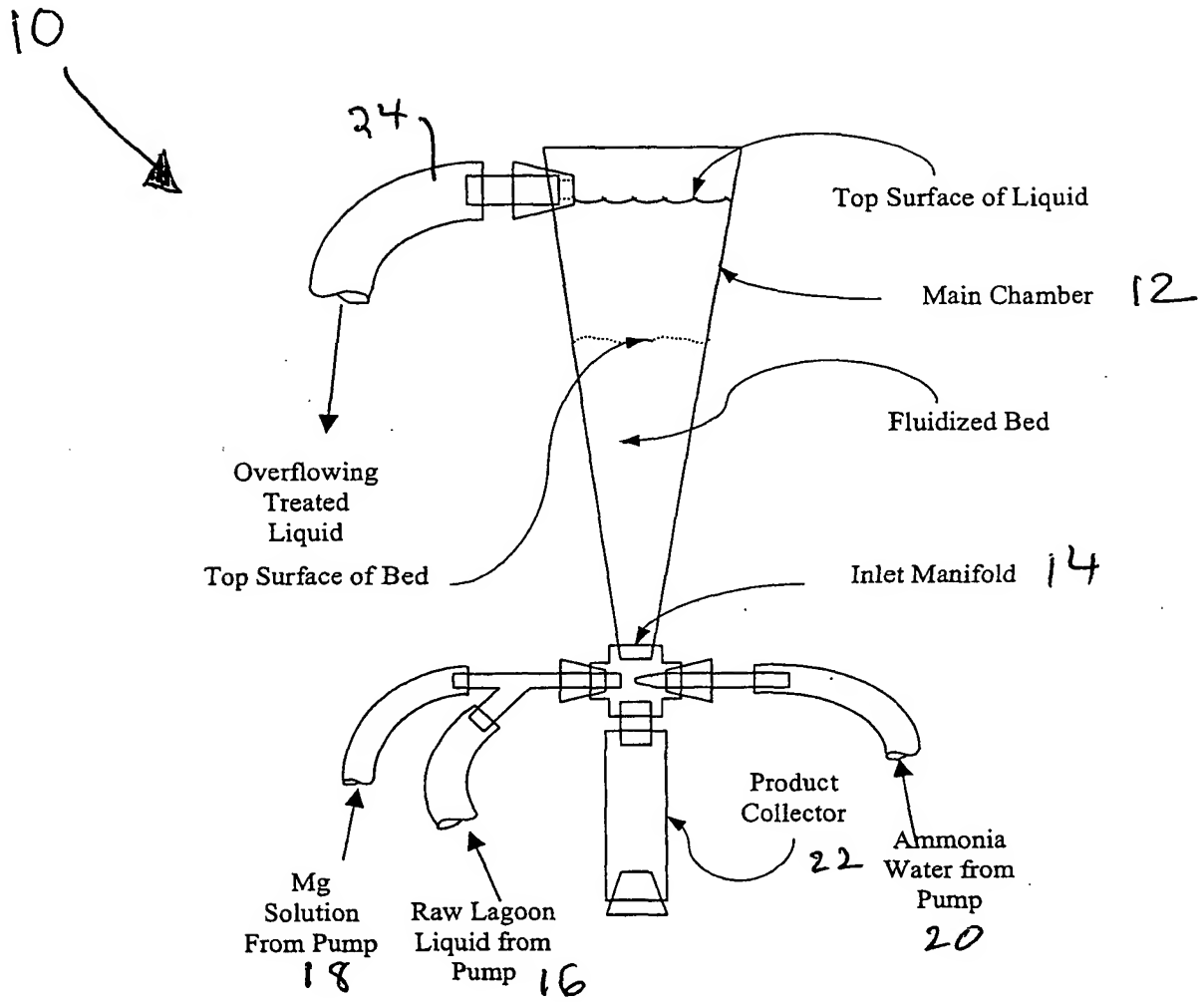

Figure 1: Sketch of Laboratory-Scale Continuous Crystallizer

Title: APPARATUS AND METHOD FOR REMOVING PHOSPHORUS FROM WASTE LAGOON EFFLUENT
Applicant(s): Bowers et al.
Atty. Docket No.: 297/181

Figure 11A

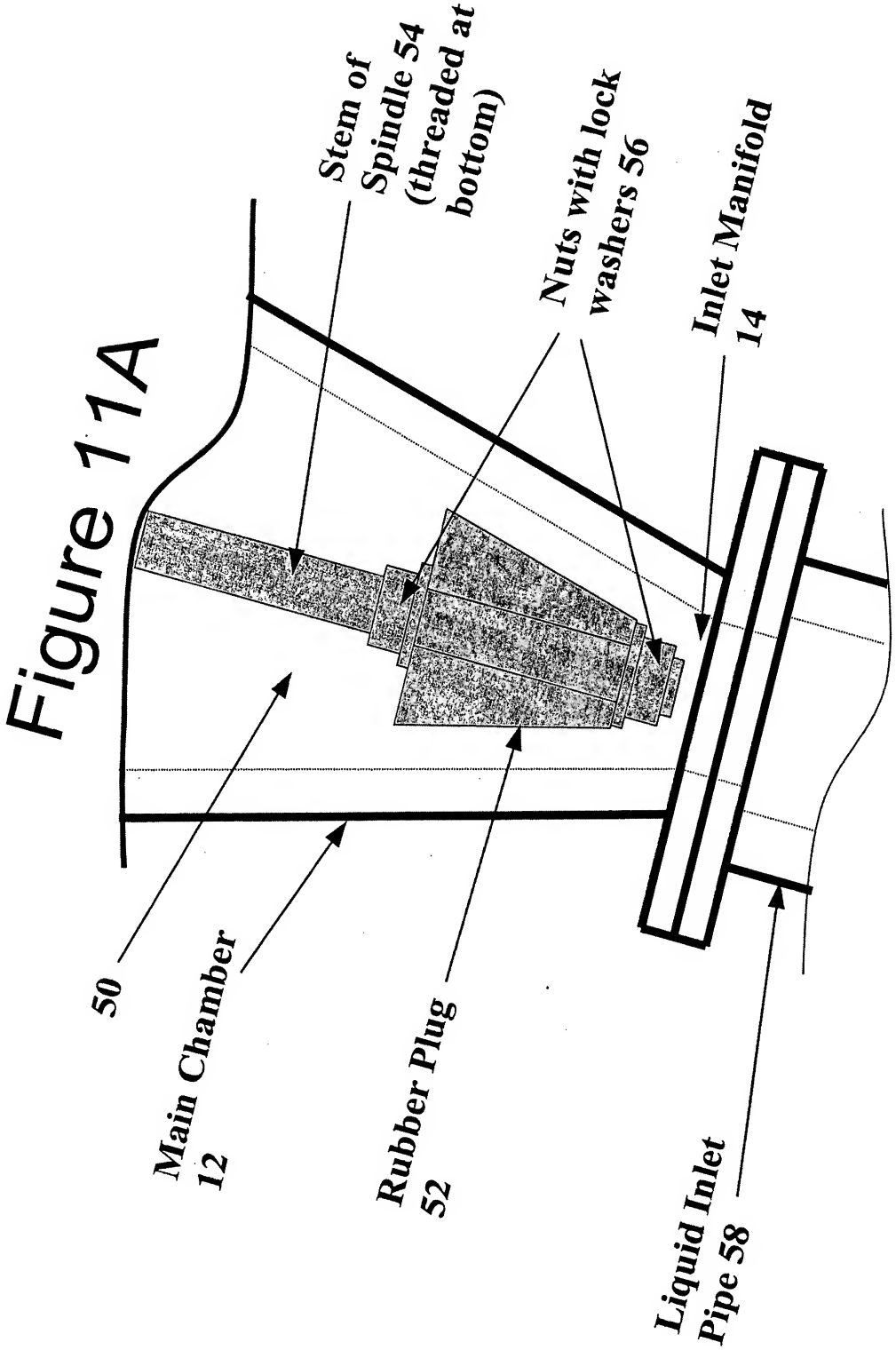

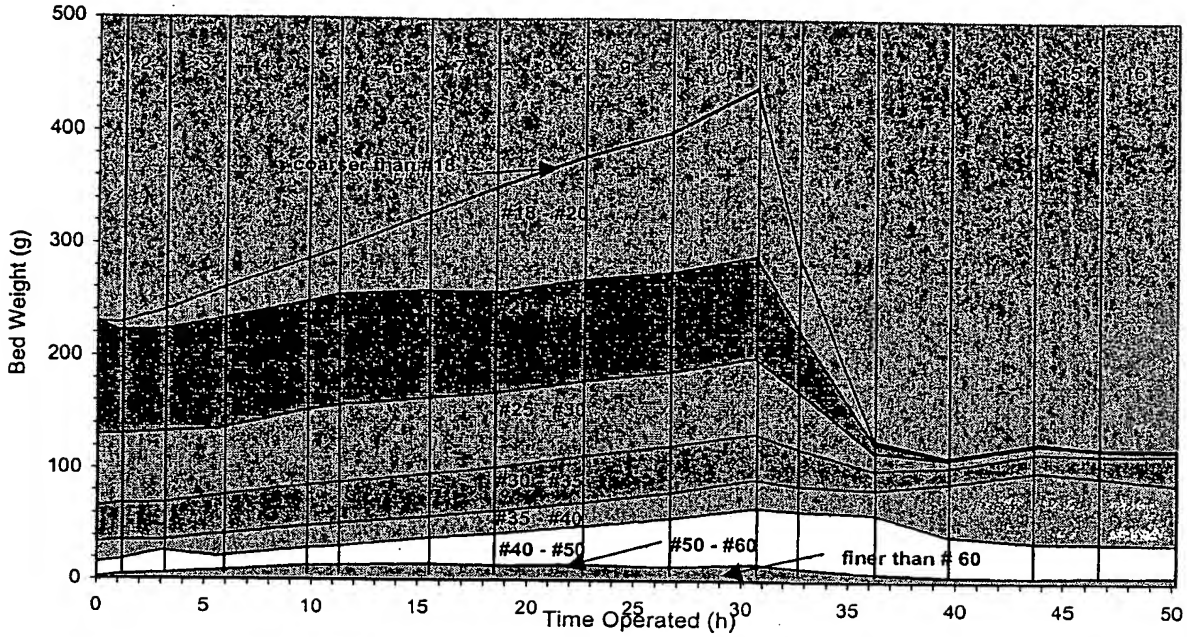

Figure 12: First Series of FCRs: Bed Weight (g), Broken Down by Particle Size (Standard Sieve), vs. Time Operated (h)
(Numbered Vertical Strips Correspond with Runs)

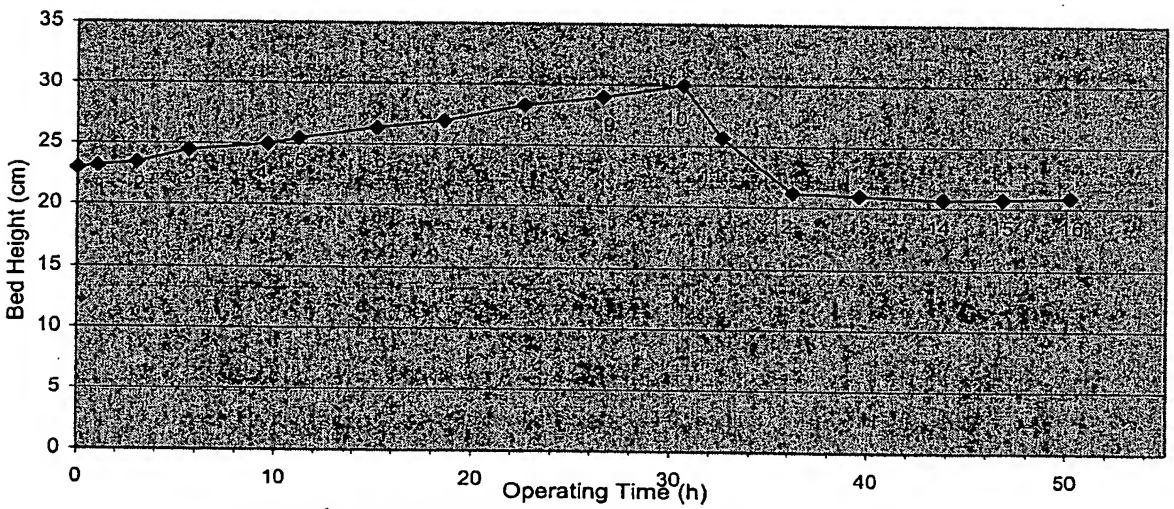

Figure 13: First Series of FCRs: Bed Height (cm) at End of Run vs. Operating Time (h)
(Run Numbers Indicated)

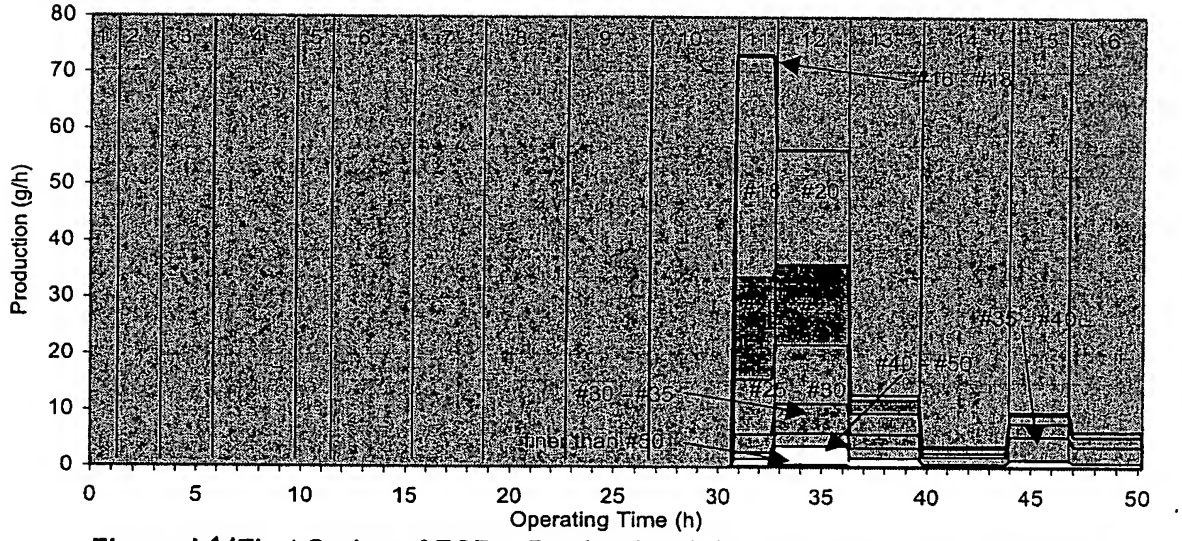

Figure 14: First Series of FCRs: Production (g/h), Averaged Over Each Run, Broken Down by Particle Size (Standard Sieve)
(Numbered Vertical Strips Correspond with Runs)

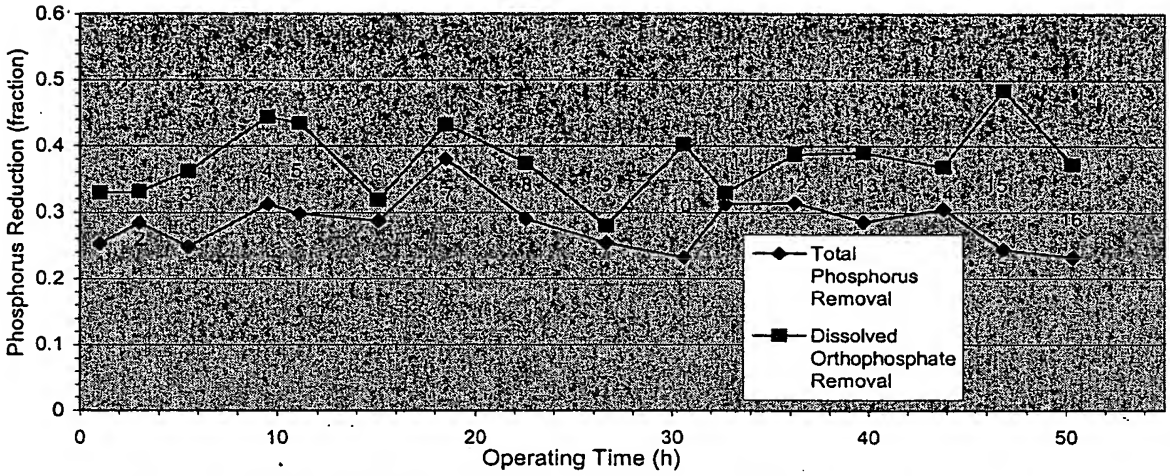

Figure 15: First Series of FCRs: Phosphorus Reduction (fraction) vs. Operating Time (h)
(Run Numbers Indicated)

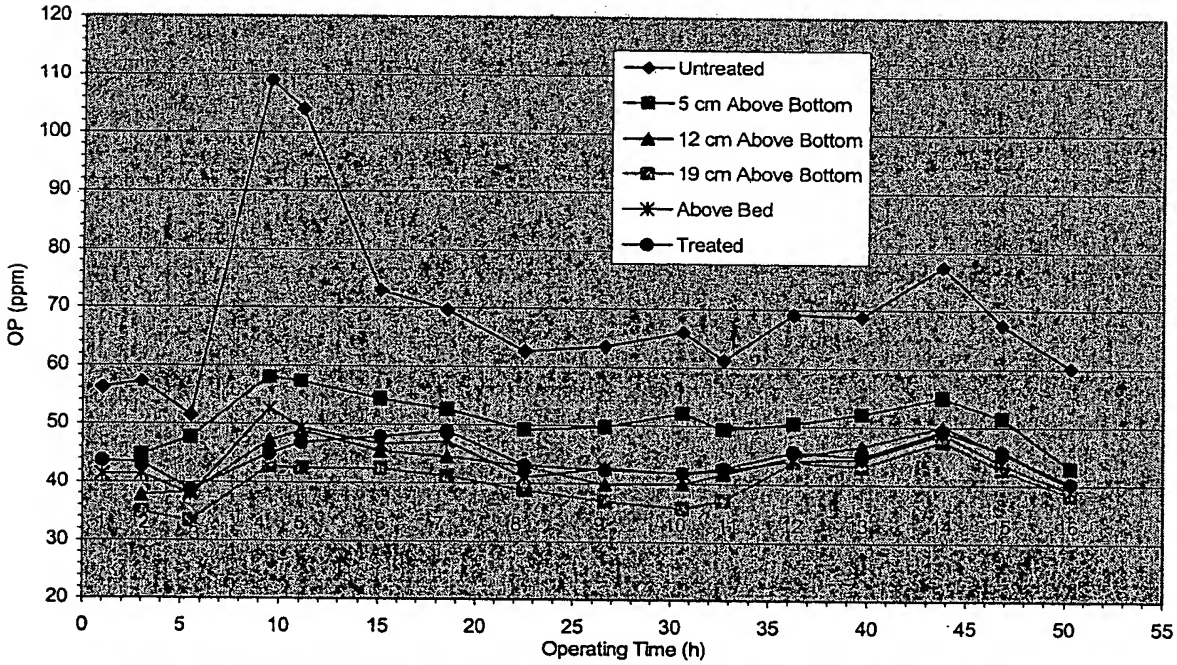

Figure 16: First Series of FCRs: OP (ppm) at Various Sampling Points vs. Operating Time (h)
(Run Numbers Indicated)

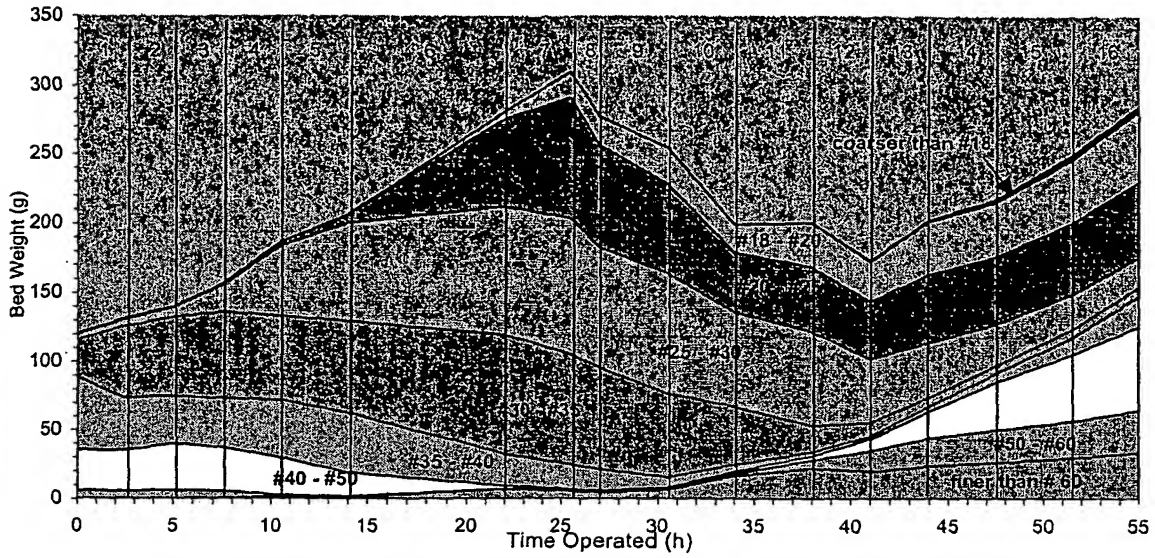

Figure 17: Second Series of FCRs: Bed Weight (g), Broken Down by Particle Size (Standard Sieve), vs. Time Operated (h)
(Numbered Vertical Strips Correspond with Runs)

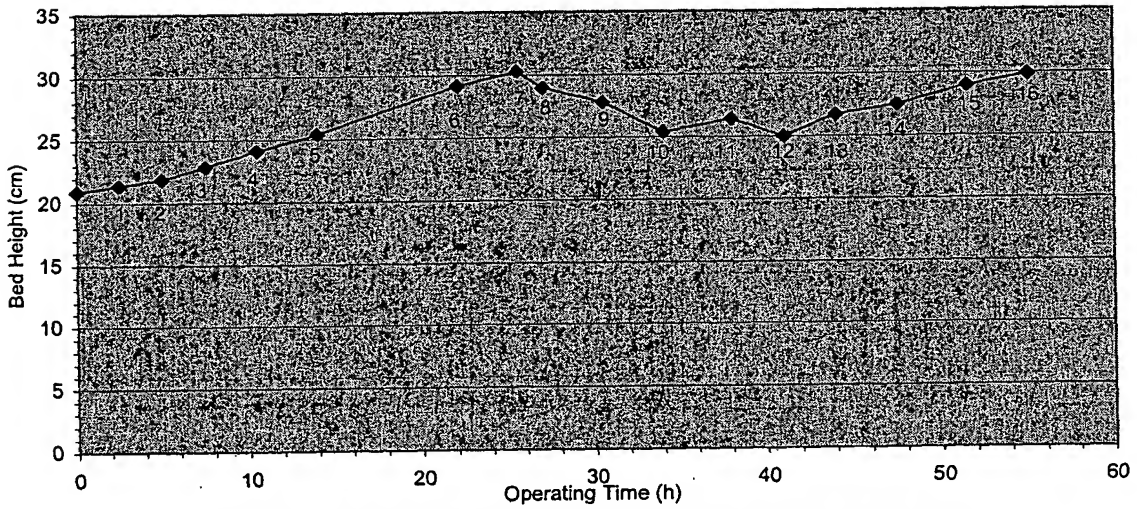

Figure 18: Second Series of FCRs: Bed Height (cm) at End of Run vs. Operating Time (h)
(Run Numbers Indicated)

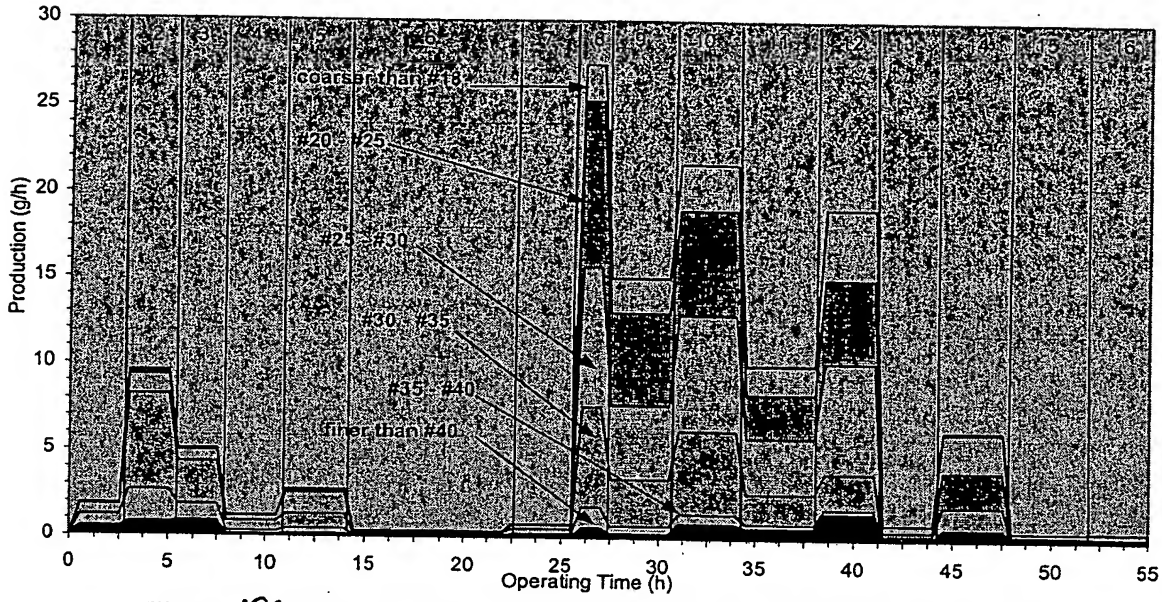

Figure 19: Second Series of FCRs: Production (g/h), Averaged Over Each Run, Broken Down by Particle Size (Standard Sieve)
(Numbered Verticle Strips Correspond with Runs)

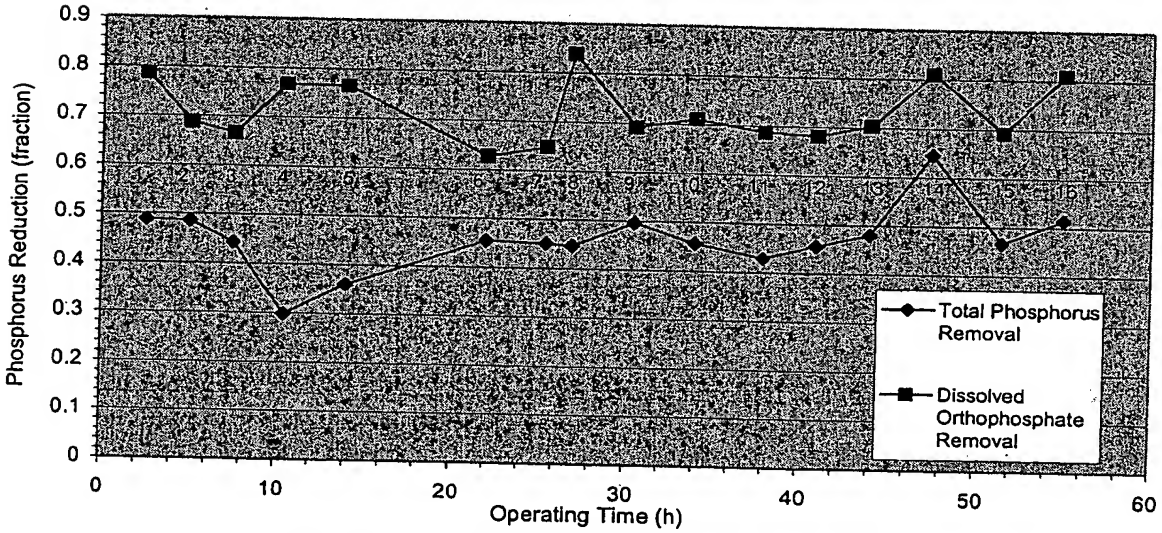

Figure 20: Second Series of FCRs: Phosphorus Reduction (fraction) vs. Operating Time (h)
(Run Numbers Indicated)

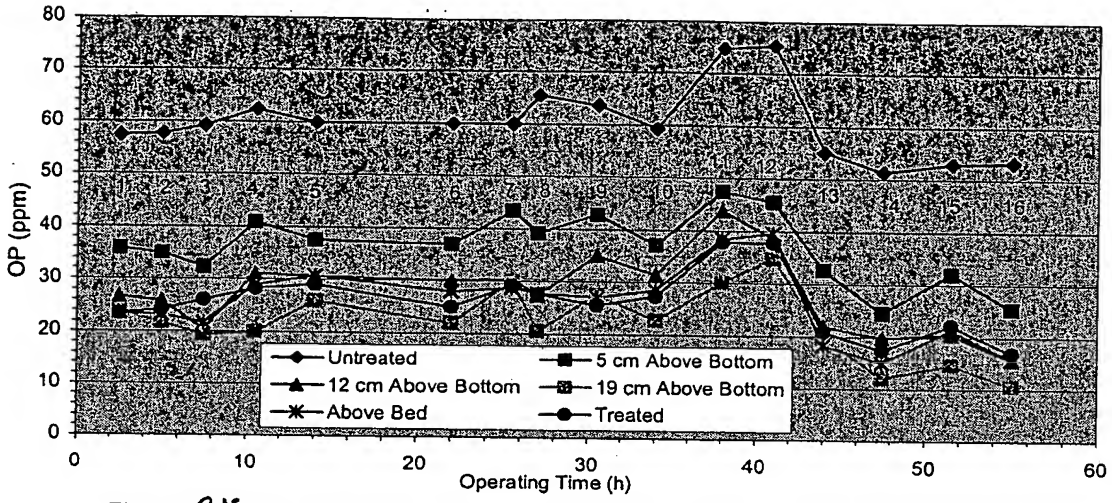

Figure 21: Second Series of FCRs: OP (ppm) at Various Sampling Points vs. Operating Time (h)
(Run Numbers Indicated)

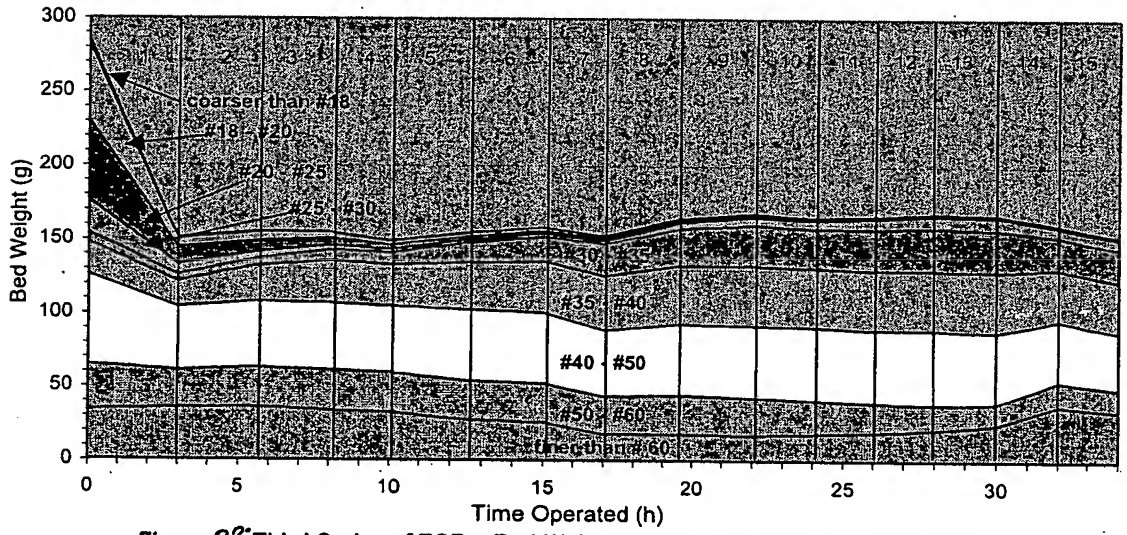

Figure 22: Third Series of FCRs: Bed Weight (g), Broken Down by Particle Size (Standard Sieve), vs. Time Operated (h)
(Numbered Vertical Strips Correspond with Runs)

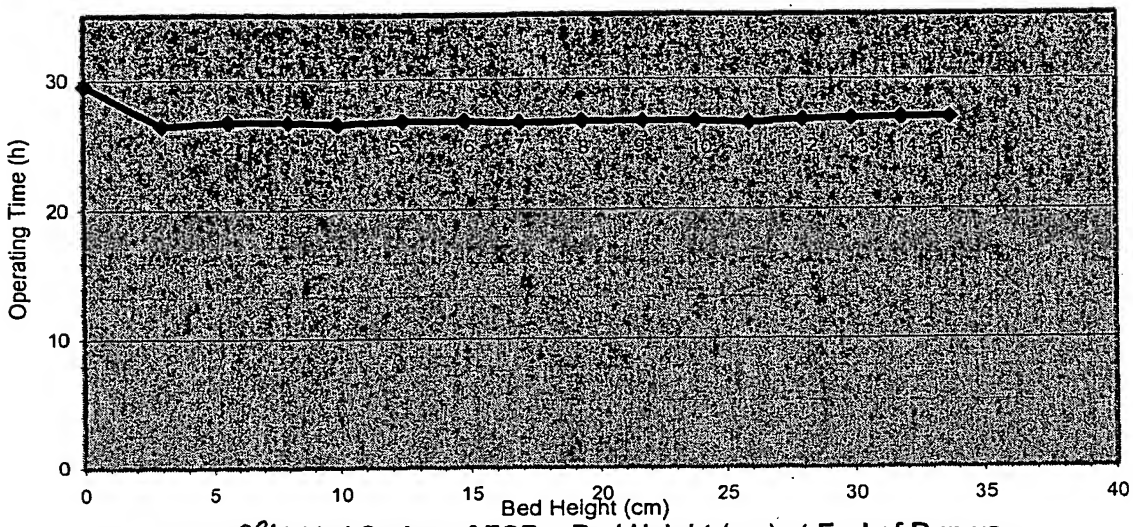

Figure 23: Third Series of FCRs: Bed Height (cm) at End of Run vs. Operating Time (h)
(Run Numbers Indicated)

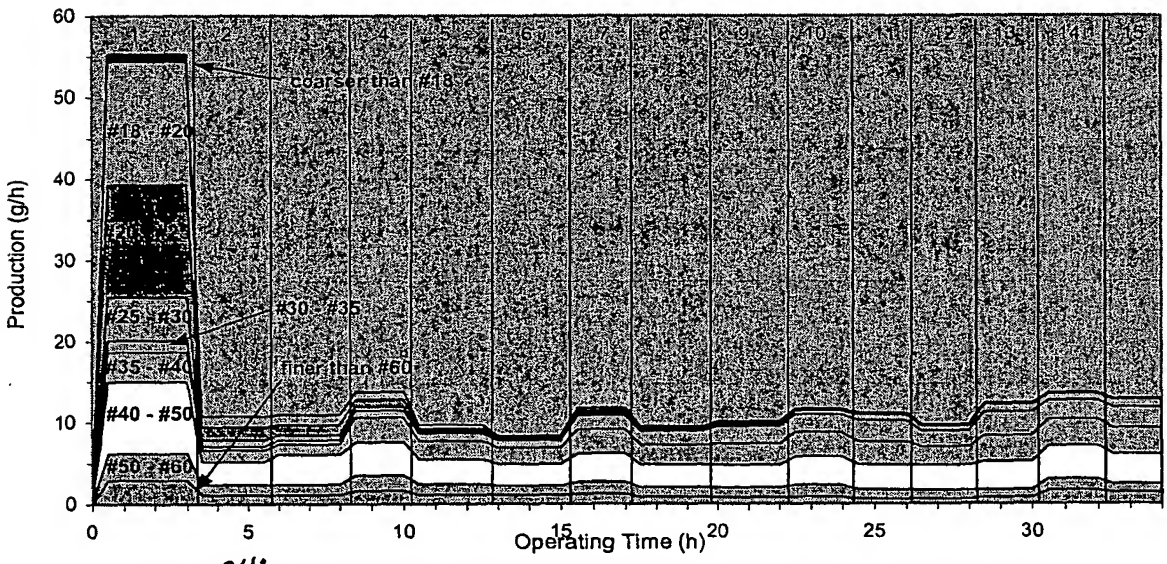

Figure 24: Third Series of FCRs: Production (g/h), Averaged Over Each Run, Broken Down by Particle Size (Standard Sieve)
(Numbered Vertical Strip Correspond with Runs)

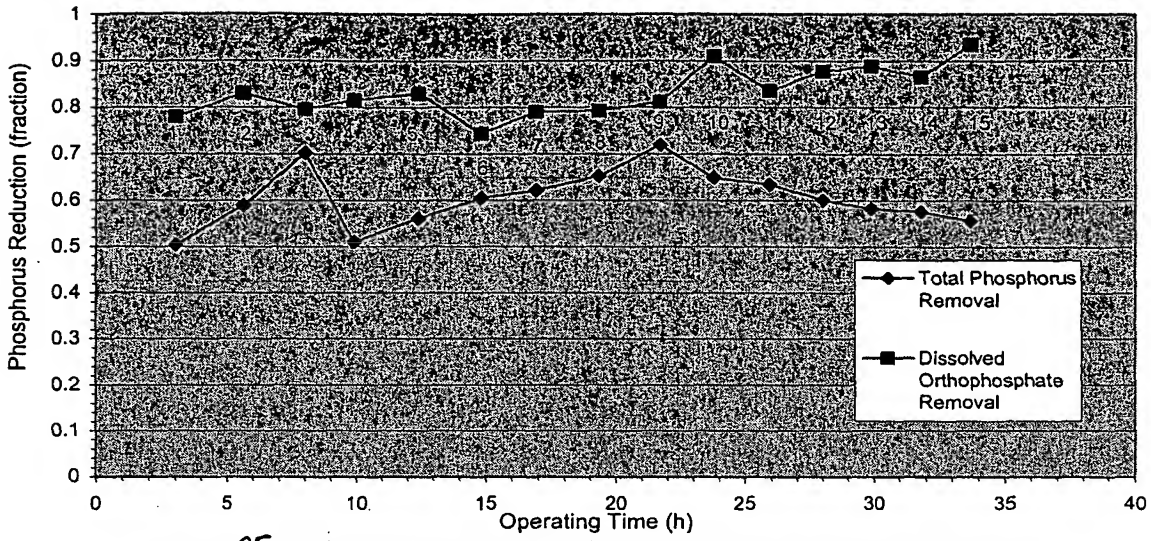

Figure 25: Third Series of FCRs: Phosphorus Reduction (fraction) vs. Operating Time (h)
(Run Numbers Indicated)

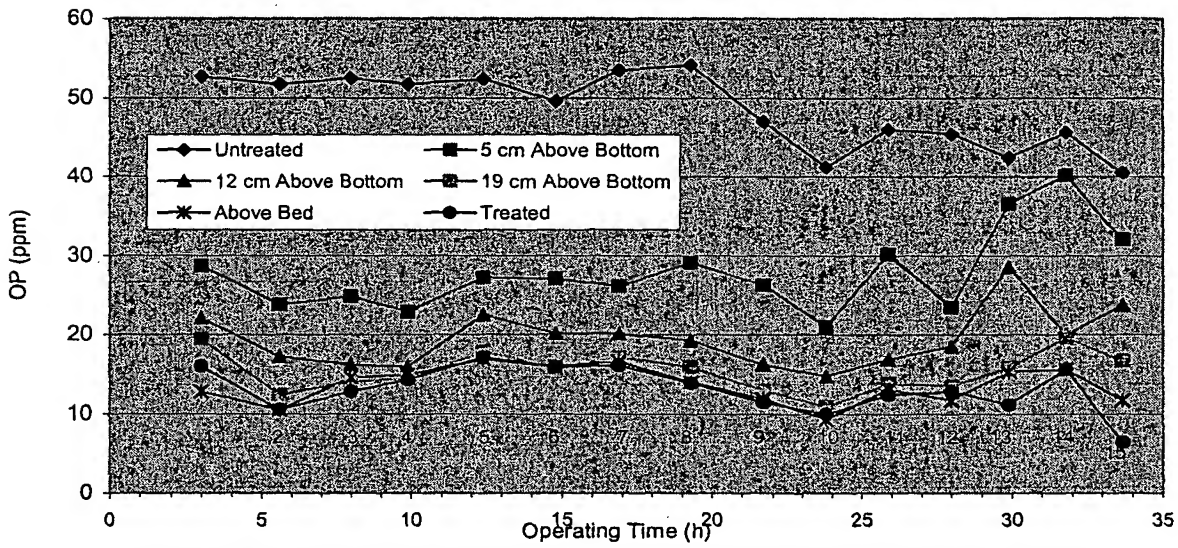

Figure 26: Third Series of FCRs: OP (ppm) at Various Sampling Points vs. Operating Time (h)
(Run Numbers Indicated)

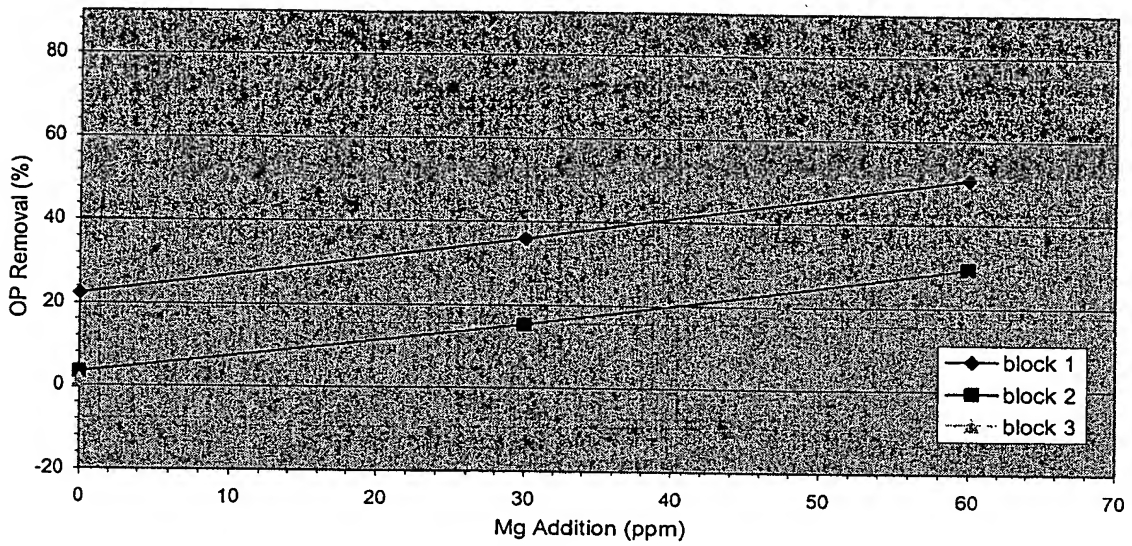

Figure 27: MVRs: OP Removal (%) vs. Mg Addition (ppm) with Zero Ammonia and 41.2 L/h Flow

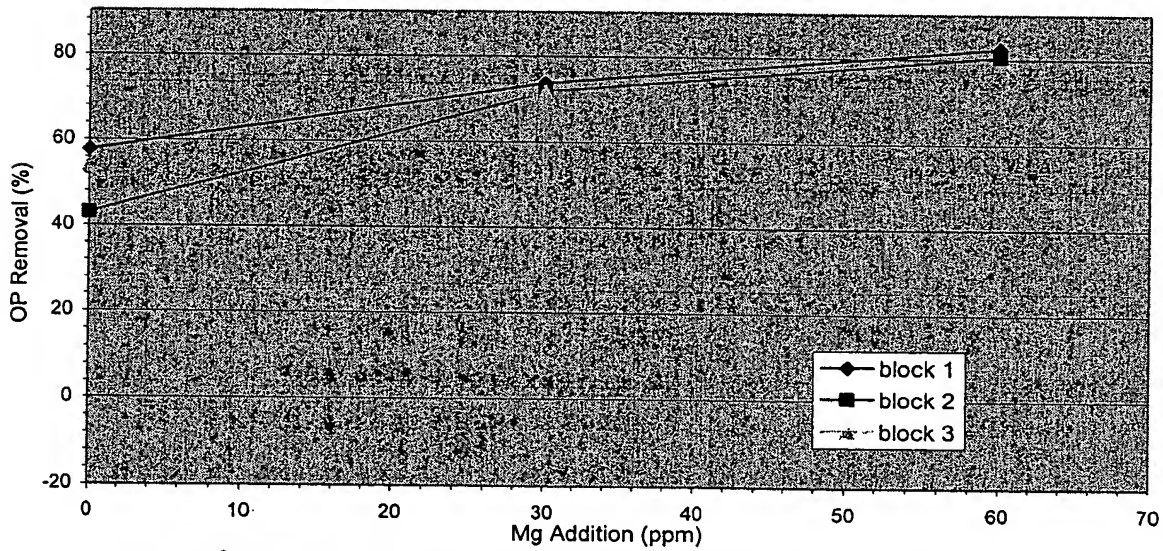

Figure 28: MVRs: OP Removal (%) vs. Mg Addition (ppm) with 100 ppm (as TAN) Ammonia Addition and 41.2 L/h Flow

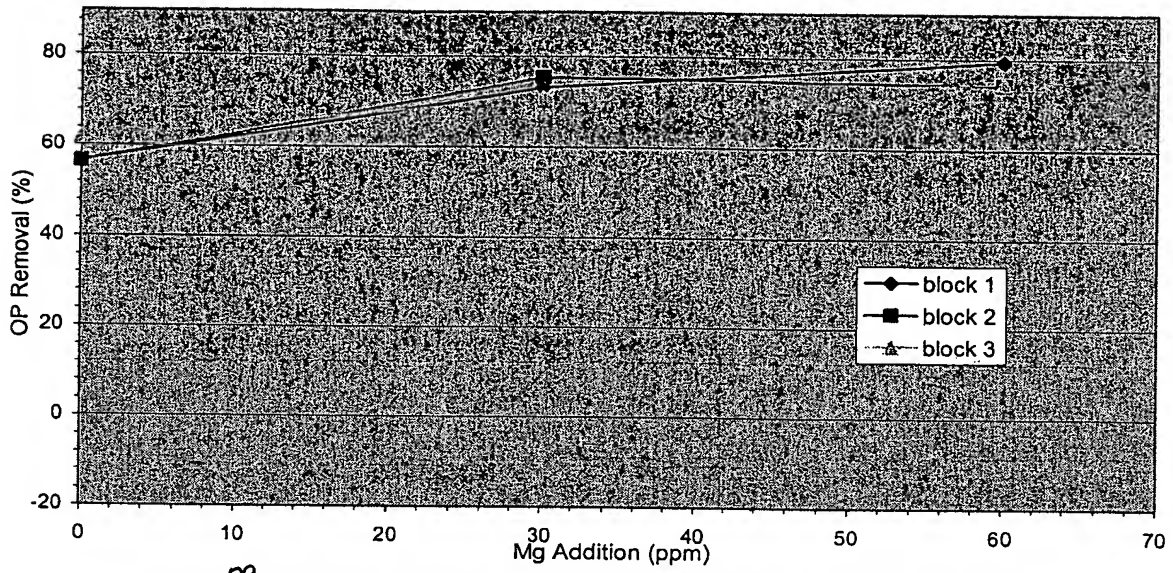

Figure 29: MVRs: OP Removal (%) vs. Mg Addition (ppm) with 200 ppm (as TAN) Ammonia and 41.2 L/h Flow

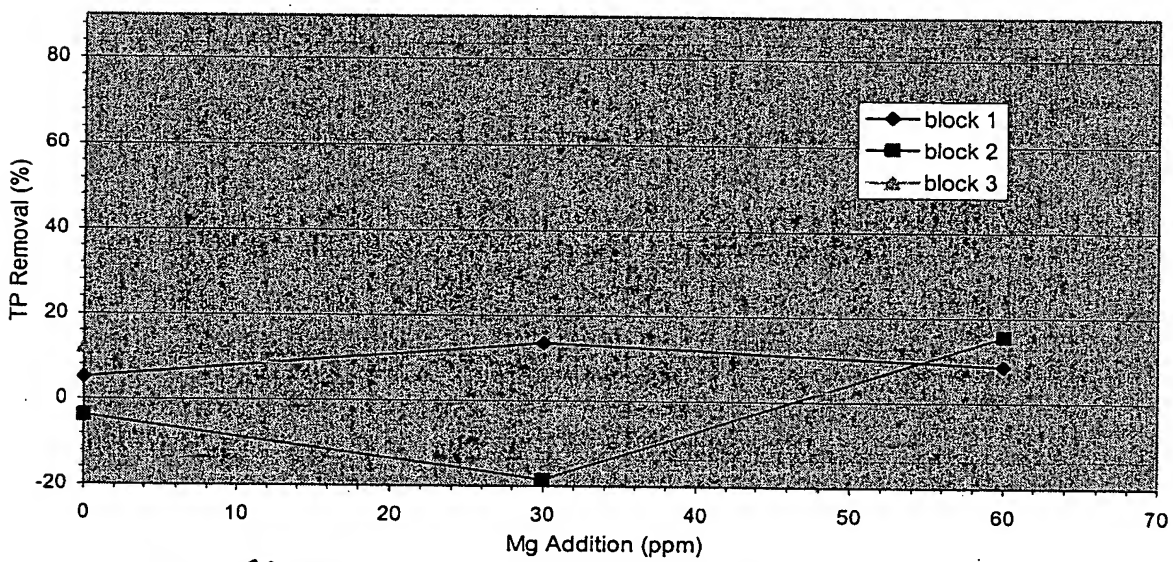

Figure 30: MVRs: TP Removal (%) vs. Mg Addition (ppm) with Zero Ammonia and 41.2 L/h Flow

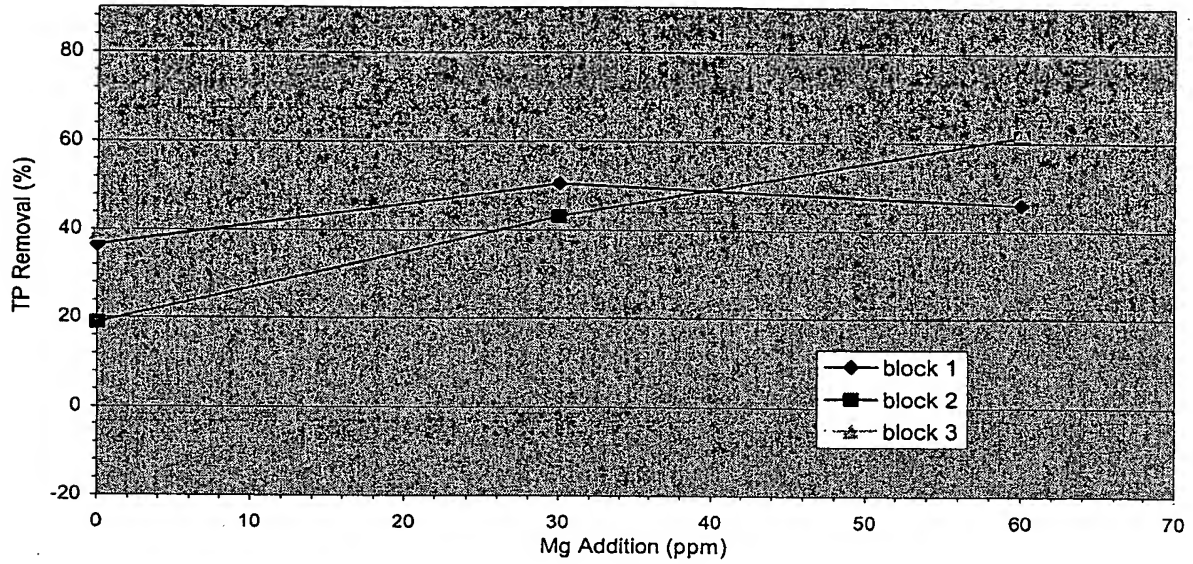

Figure 31: MVRs: TP Removal (%) vs. Mg Addition (ppm) with 100 ppm (as TAN) Ammonia and 41.2 L/h Flow

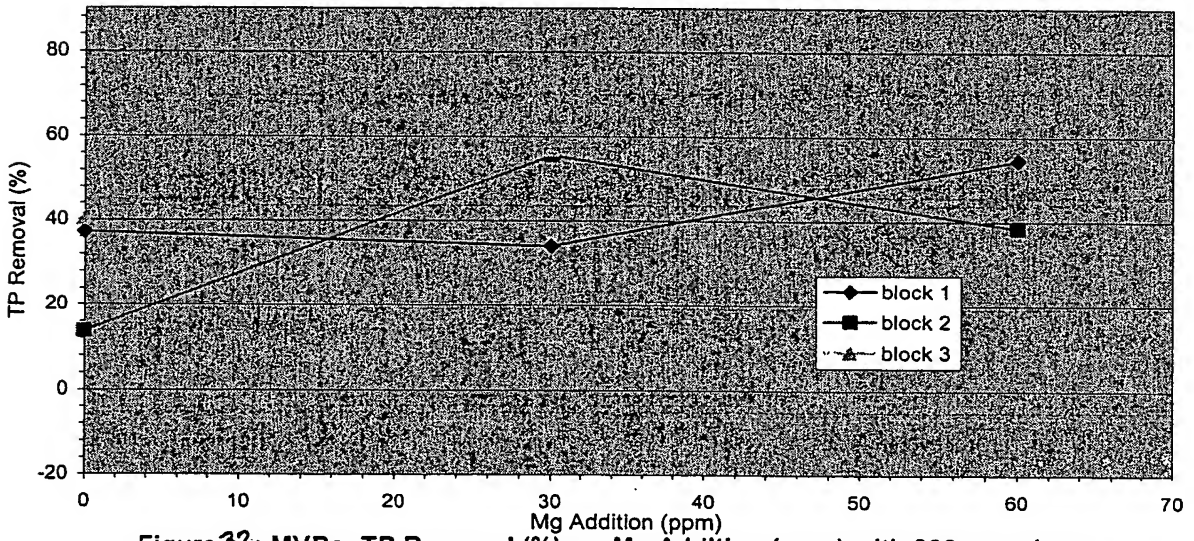

Figure 32: MVRs: TP Removal (%) vs. Mg Addition (ppm) with 200 ppm (as TAN) Ammonia and 41.2 L/h Flow

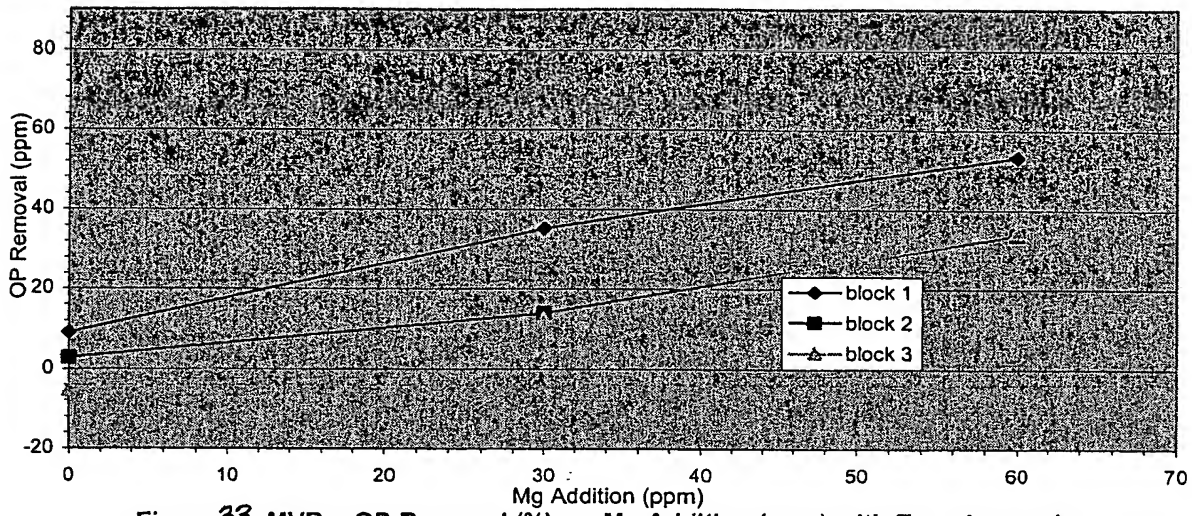

Figure 33: MVRs: OP Removal (%) vs. Mg Addition (ppm) with Zero Ammonia and 56.8 L/h Flow

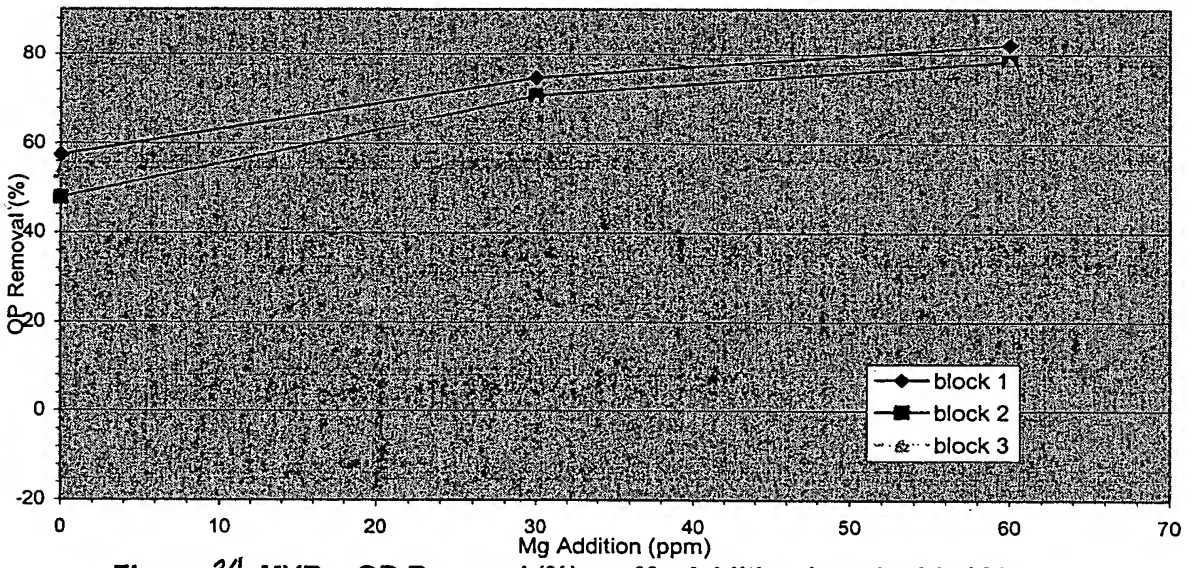

Figure 34: MVRs: OP Removal (%) vs. Mg Addition (ppm) with 100 ppm (as TAN) Ammonia and 56.8 L/h Flow

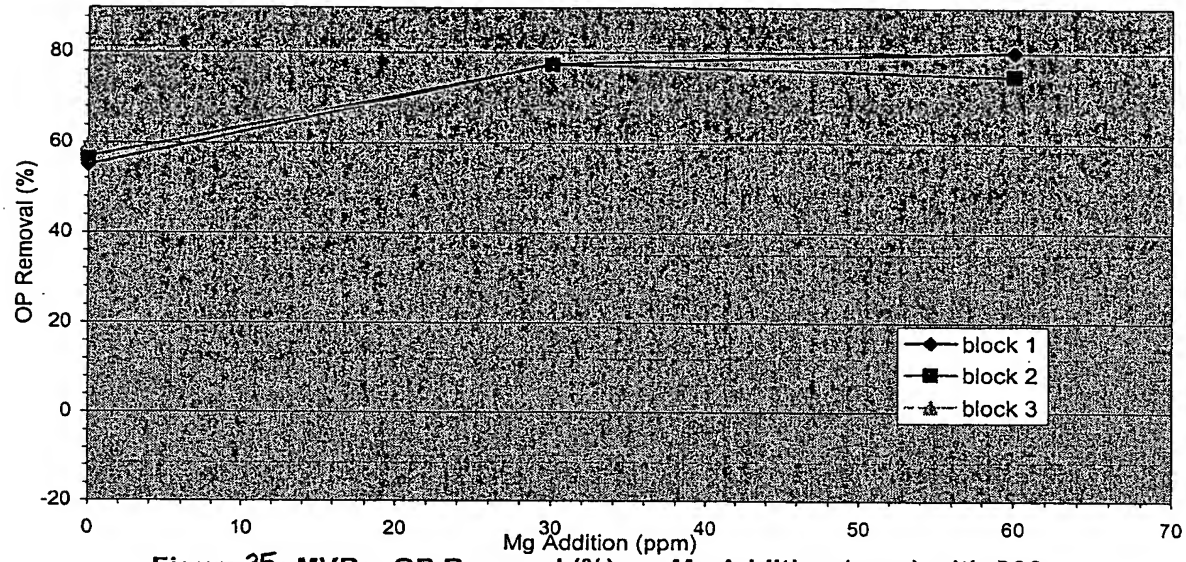

Figure 35: MVRs: OP Removal (%) vs. Mg Addition (ppm) with 200 ppm (as TAN) Ammonia and 56.8 L/h Flow

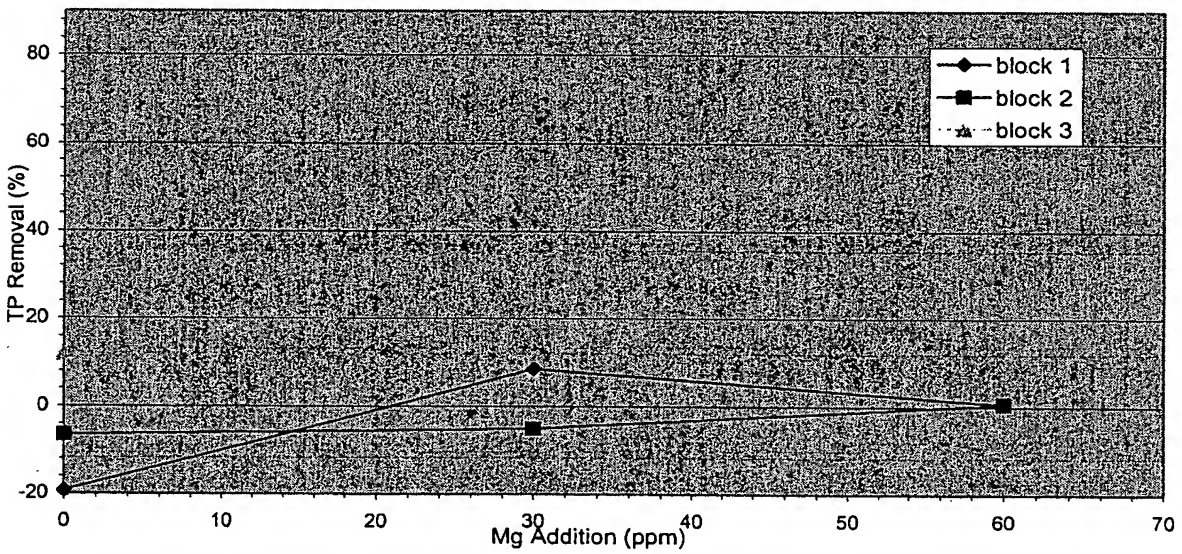

Figure 36: MVRs: TP Removal (%) vs. Mg Addition (ppm) with Zero Ammonia and 56.8 L/h Flow

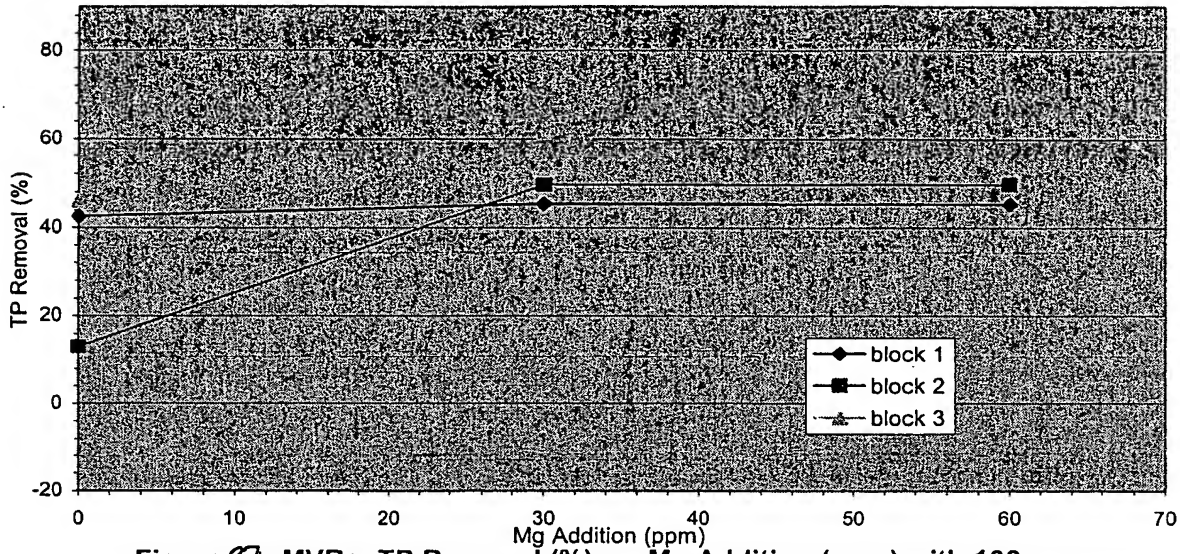

Figure 37: MVRs: TP Removal (%) vs. Mg Addition (ppm) with 100 ppm (as N) Ammonia and 56.8 L/h Flow

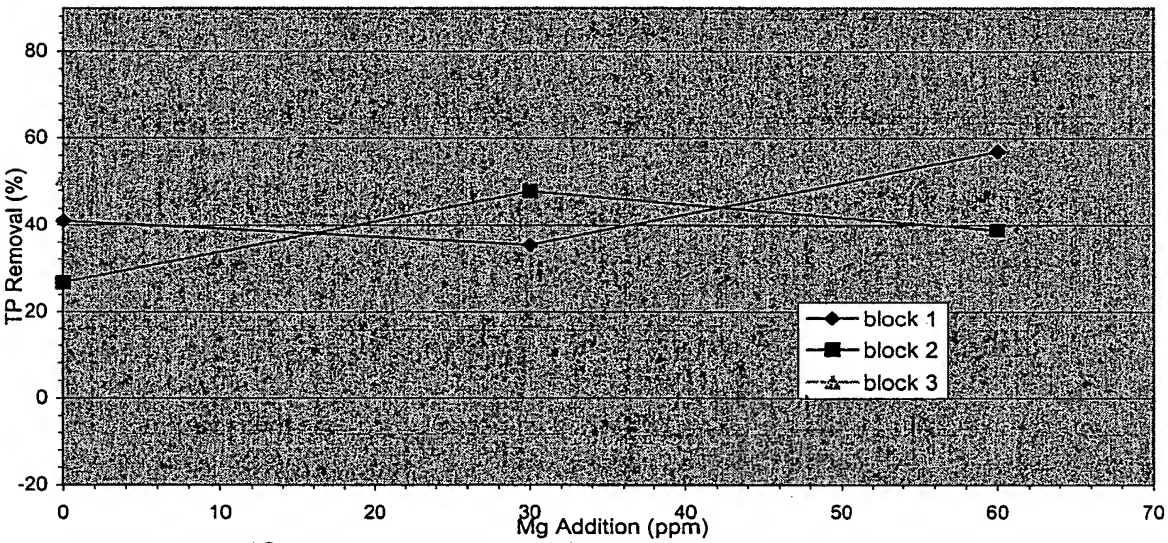

Figure 38: MVRs: TP Removal (%) vs. Mg Addition (ppm) with 200 ppm (as N) Ammonia and 56.8 L/h Flow

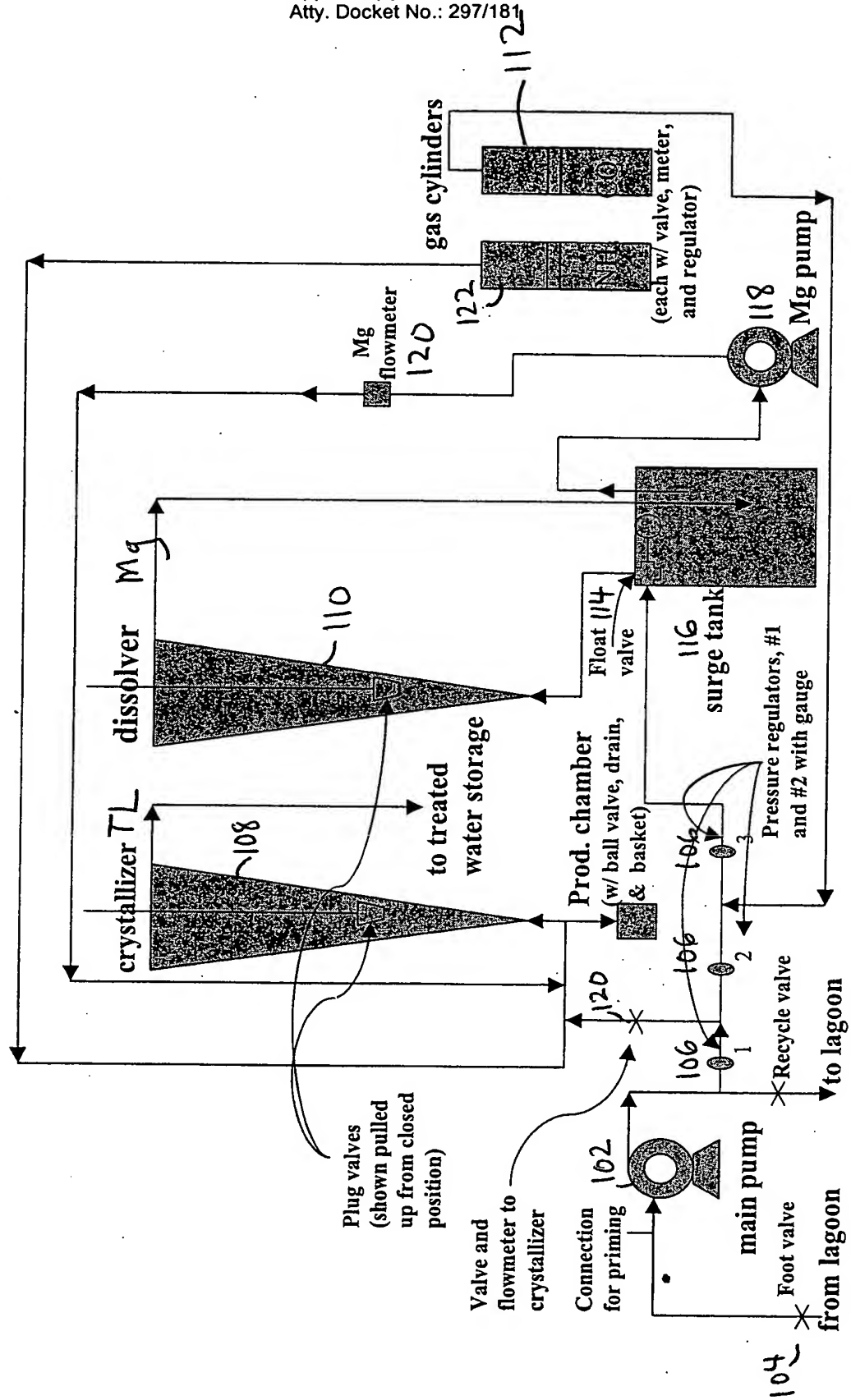

Figure 3: Schematic Representation of Field-Scale Crystallizer, Showing Principal Components

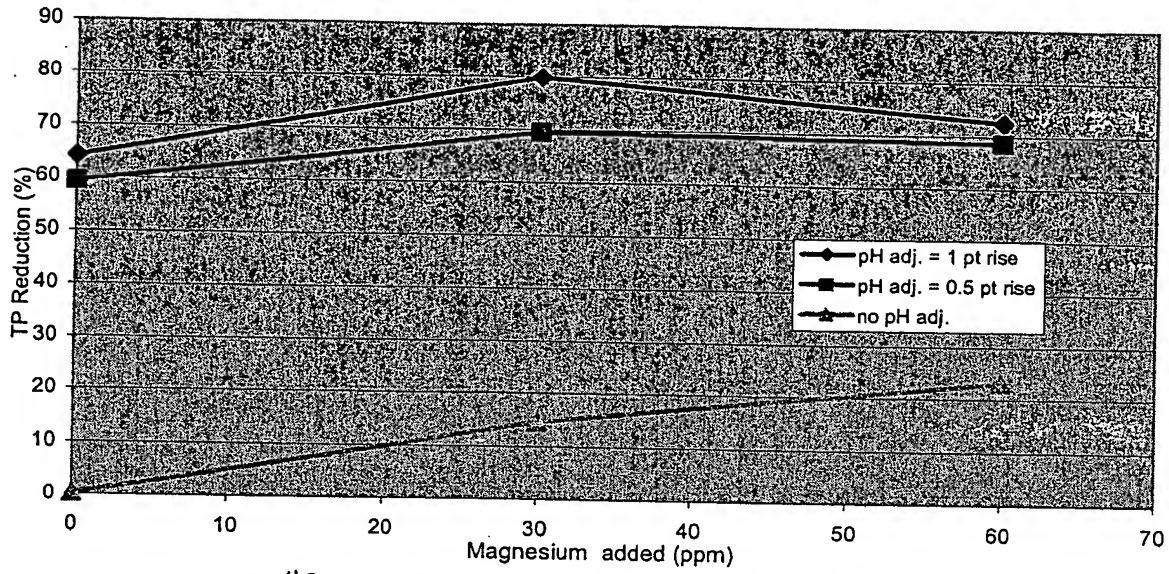

Figure 40: TP Reduction (%) vs. Magnesium added (ppm) at Lower Flow Rate (341 L/h)

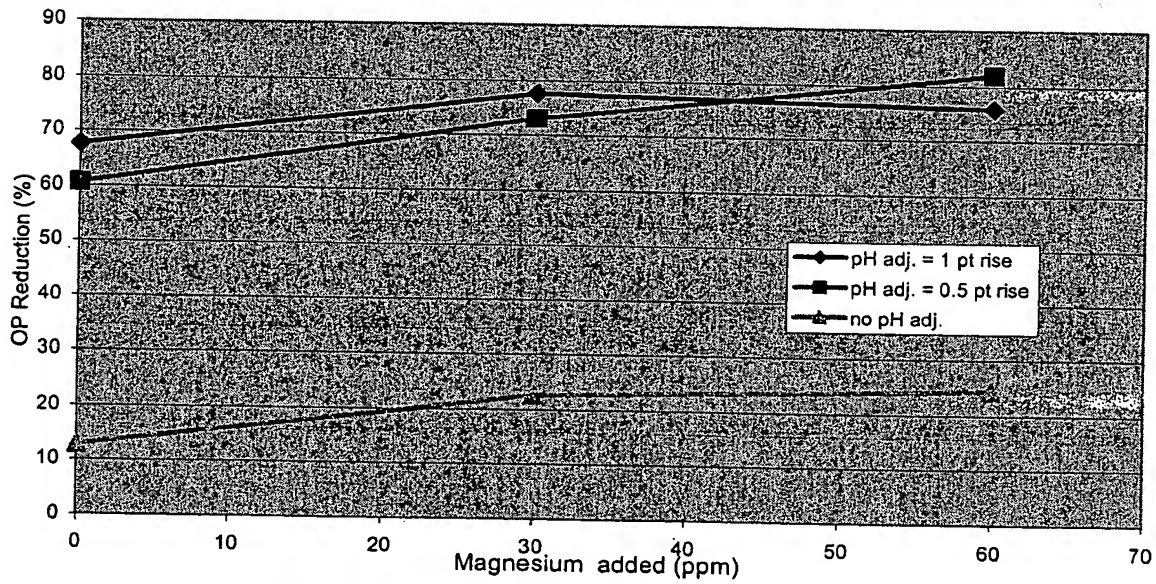

Figure 41: OP Reduction (%) vs. Magnesium added (ppm) at Lower Flow Rate (341 L/h)

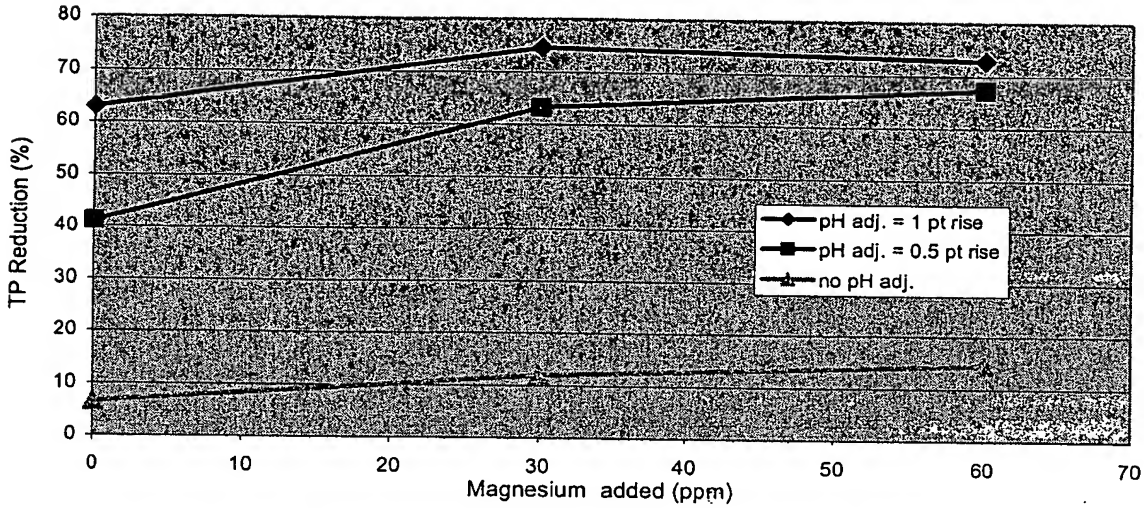

Figure 42: TP Reduction (%) vs. Magnesium added (ppm) at Higher Flow Rate (568 L/h)

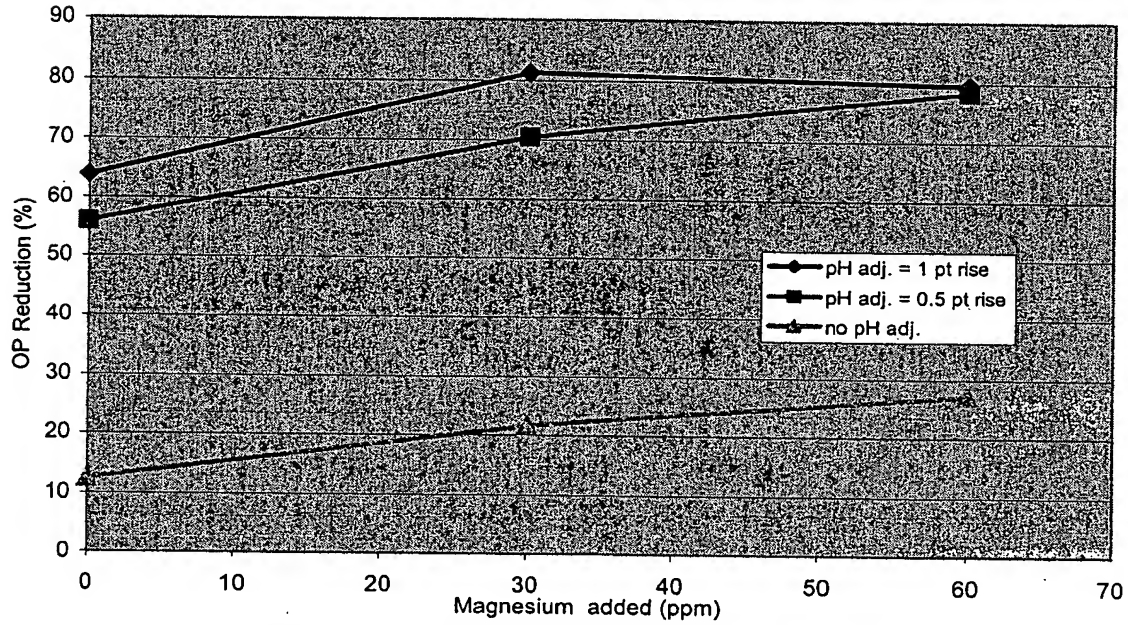

Figure 43: OP Reduction (%) vs. Magnesium added (ppm) at Higher Flow Rate (568 L/h)